Pharm Res (2011) 28:2191–2203
DOI 10.1007/s11095-011-0447-0

RESEARCH PAPER

Molecular Motions in Sucrose-PVP and Sucrose-Sorbitol Dispersions: I. Implications of Global and Local Mobility on Stability

Sisir Bhattacharya • Raj Suryanarayanan

Received: 24 December 2010 / Accepted: 5 April 2011 / Published online: 18 April 2011

ABSTRACT

Purpose To characterize molecular mobility by dielectric spectroscopy and determine the effect of additives on α- and β-relaxation times in amorphous sucrose solid dispersions.

Methods Sucrose was co-lyophilized with either PVP or sorbitol. The lyophiles were subjected to dielectric spectroscopy and differential scanning calorimetry.

Results The additives did not have an appreciable effect on the calorimetric T_g. However, dielectric spectroscopy revealed pronounced effects on global mobility (α-relaxation), which correlated with the crystallization tendency of sucrose. The systems were characterized by two β-relaxations, and the relaxation times as well as their temperature dependence were influenced by the additive. Although sorbitol acted as a plasticizer of sucrose with respect to global mobility, it anti-plasticized sucrose in terms of local motions. PVP, on the other hand, acted as an anti-plasticizer with respect to both global and local mobility. The slower β-relaxation in amorphous sucrose was found to correlate with the α-relaxation and was identified as the Johari-Goldstein relaxation.

Conclusions Amorphous systems with identical calorimetric T_g could have significantly different mobility and physical stability as revealed by dielectric spectroscopy. Additive effect on global mobility cannot be a predictor of the effects on local mobility. Additives could also be used to inhibit local mobility.

S. Bhattacharya • R. Suryanarayanan (✉)
Department of Pharmaceutics University of Minnesota
Minneapolis, Minnesota 55455, USA
e-mail: surya001@umn.edu

Present Address:
S. Bhattacharya
Forest Research Institute Forest Laboratories, Inc.
49 Mall Drive,
Commack, New York 11725, USA

KEY WORDS amorphous · dielectric spectroscopy · global and local mobility · solid dispersions · sucrose

INTRODUCTION

The development of active pharmaceutical ingredients in the amorphous state is increasingly recognized as a means to circumvent the challenges of poor aqueous solubility and consequently the slow dissolution rate of compounds (1). However, the increased free energy of the amorphous state can also result in a decreased physical stability, manifested by the tendency to crystallize. Similarly, a decreased chemical stability can lead to an unacceptably short shelf-life. Therefore, current research efforts are directed towards predicting the stability of amorphous pharmaceuticals (2–6).

The possible coupling between molecular motions and the stability of amorphous phases is deservedly receiving a lot of attention from pharmaceutical researchers. The molecular motions bringing about glass transition are referred to as global mobility (also known as α- or primary relaxation), an important and characteristic property of amorphous materials, which may be directly related to the issues of potential physicochemical instability. Expectedly, in the last two decades, much effort has been directed towards studying glass transition and the implications of the underlying molecular mobility (7–10). However, the glass transition temperature (T_g) has not always served as a reliable predictor of the stability of amorphous pharmaceuticals (11–13). In these instances, the observed instability was attributed to local mobility (explained in the next paragraph). There is evidence in the literature of local motions being directly responsible for crystallization in amorphous systems (14–18). A sudden increase in crystal growth has been observed in some small molecule organic compounds at temperatures close to T_g

(14–18). In these cases, crystallization kinetics were not controlled by self-diffusion coefficient. The rapid crystallization could not be explained based on the primary relaxation time and was attributed to "local motions."

Glassy systems have been shown to have local intermolecular or intramolecular reorientations known as β- or secondary relaxations or "local mobility" (19). As opposed to α-relaxations, these are non-cooperative and much faster, with the relaxation time being typically $<10^{-1}$ s at the glass transition temperature. In contrast to α-relaxations, the β-relaxations generally obey Arrhenius kinetics and are characterized by activation energy values that are much lower than those of α-relaxations (20,21). Intramolecular motions involve the movement of only a part of the molecule, e.g., polymer side chains. Non-cooperative secondary relaxations, argued to involve the motion of entire molecule, were shown to be universally present in both rigid and non-rigid organic small molecule glasses by Johari and Goldstein and hence have come to be known as the Johari-Goldstein (JG) relaxations (22). JG relaxations are thought to be fundamentally important because they have been argued to be the precursor to the cooperative α-relaxation and have been explained by the extended coupling model of Ngai (23). Thus, even if local mobility is not directly responsible for instability in an amorphous matrix, it could indirectly destabilize the amorphous system by facilitating global mobility.

Until recently, pharmaceutical researchers have mostly neglected local mobility because its role as a precursor of glass transition was not readily recognized. Moreover, the potential role of local motions in bringing about instability in the amorphous state, particularly crystallization, was poorly understood. In addition, molecular mobility below T_g was measured indirectly from studies above T_g (24). However, information on the mobility below T_g, derived by extrapolation from the data obtained above T_g, is inadequate to explain the local mobility or the non-cooperative β-relaxations (25), which persist well below the T_g (21). In order to understand the role of molecular mobility on stability, it is necessary to look beyond glass transition, directly characterize local mobility, and investigate the relationship between local and global mobility.

Pharmaceutical formulations are often miscible amorphous mixtures of multiple components, as in solid dispersions manufactured by different techniques such as spray drying, lyophilization and hot melt extrusion. Assuming molecular motions are coupled to physical stability, the molecular mobility and hence crystallization tendency of the component of interest can be influenced by the other components in the system. Investigation of changes in the molecular dynamics in binary amorphous pharmaceutical systems would help us understand the implications of additives on crystallization of the compounds of interest.

We have used model amorphous systems in order to characterize global and local mobility and investigate their relationship. Specifically, amorphous sucrose was used as the model compound, and solid dispersions were prepared using either poly(vinyl pyrrolidone) (PVP K90) or sorbitol. PVP (T_g of ~172°C) served as an anti-plasticizer of amorphous sucrose (T_g of ~74°C) while sorbitol (T_g of ~−2°C) was a plasticizer. Here, "plasticization" refers to an increase in global mobility in an amorphous system brought about by a lower T_g additive, while "anti-plasticization" describes the opposite effect, i.e., a decrease in global mobility by an additive with a higher T_g. Polymers such as PVP are frequently used to prepare amorphous solid drug dispersions, whereas plasticizers like sorbitol are often included to improve processability during solid dispersion manufacture. The plasticizing and anti-plasticizing effects of additives on global mobility in an amorphous pharmaceutical are well documented (8). However, we have an incomplete understanding of the local mobility in pharmaceutical molecular dispersions containing a plasticizer or an anti-plasticizer.

In light of the earlier discussions, it is also important to study the correlations between the local and global mobility in such binary systems. In order to retain virtually the same glass transition temperature, the additive concentration was fixed at 2.5% w/w of the total solids in the system. Different grades of PVP, even at low concentrations, have been shown to inhibit sucrose crystallization with the high molecular weight PVP being the most effective (26). Interestingly, the glass transition temperature was unaffected by the addition of PVP (27). The virtually identical calorimetric T_g values were interpreted to indicate identical global mobility, and the inhibitory effects of PVP on sucrose crystallization were attributed to local motions (28). In amorphous pharmaceuticals, the relaxation time at calorimetric T_g is generally assumed to be 100 s (6). However, such an assumption is not universally valid, and a relaxation time of ~3 s was observed for amorphous sucrose (2) and trehalose (20). Calorimetric methods may underestimate molecular mobility in amorphous systems (29). This is primarily because the technique does not directly measure mobility but a consequence of relaxation (24,30). In contrast, dielectric spectroscopy probes the molecular motions directly and thus provides a more accurate measure of mobility. We have used dielectric spectroscopy, since it has proved to be an extremely useful tool to characterize molecular motions in amorphous compounds, both small and macromolecules (31–33). The technique involves the application of an alternating electric field with variable frequency to cause reorientation of dipoles in a sample. The reorientation of the dipoles occurs in a characteristic time called relaxation time and is a direct measure of the molecular mobility. Using dielectric spectroscopy, we propose to test the following hypothesis: the global mobility of sucrose-sorbitol system will

be markedly different from that of sucrose-PVP, in spite of their nearly identical T_g value.

At the Kauzmann temperature, which is usually estimated to be around (T_g - 50) (6,34), molecular mobility is considered to consist only of vibrational motions. Thus, (T_g - 50) has long been considered to be a temperature at which contributions from molecular motions to instability are negligible. However, physical instability has occurred or was at least facilitated upon storage at temperatures close to (T_g - 50) (11,35). The storage times were much less than the typical pharmaceutical shelf-life of two years. It is clear that if the local motions are coupled to crystallization, then storage even below (T_g - 50) could result in crystallization over the shelf-life. Faster (secondary) relaxations detected by dielectric spectroscopy are a manifestation of non-cooperative motions that persist well below the T_g. Two β-relaxations have been reported in some hydrogen bonded systems (36). One of these relaxations has been argued to be the Johari-Goldstein relaxation, i.e., involving the motion of entire molecules, and the other relaxation has been hypothesized to be resulting from hydrogen bonding interactions. Two secondary relaxations were recently reported in amorphous sucrose, (37). These authors prepared amorphous sucrose by the melt-quench method and identified the slower secondary relaxation as the Johari-Goldstein relaxation based on indirect observations. The faster secondary relaxation was attributed to hydrogen bonding interactions or motion of the constituent glucose and fructose rings of sucrose. Melt-quenching is not a desirable method for preparing amorphous sucrose, since sucrose undergoes rapid degradation upon melting (38). Nevertheless, the presence of secondary relaxations in glassy sucrose serves as a proof of significant molecular mobility at temperatures even below (T_g - 50). While the effect of polymers (used in solid dispersions) on global mobility has been extensively studied, little is known of their influence on local motions. One of our primary objectives in this study was to investigate the effect of commonly used solid dispersion additives on the local motions in binary amorphous systems. We hypothesize that PVP and sorbitol would influence the timescale of local mobility at a given temperature as well as the temperature dependence of local mobility. In addition, since the two secondary relaxations in amorphous sucrose are probably of different molecular origin, it is likely that the timescale as well as temperature dependence of each of these relaxations would be influenced differently in presence of PVP and sorbitol.

MATERIALS AND METHODS

Crystalline sucrose and sorbitol (Sigma, St. Louis, MO, USA) and PVP-K90 (Plasdone K-90, ISP Technologies Inc., Wayne, NJ, USA) were used as obtained.

Preparation of Amorphous Phases

Lyophilization of sucrose was carried out in a tray freeze-drier (Model UNITOP 400 L, Virtis, Gardiner, NY, USA). Aqueous solutions of sucrose (15% w/v), placed in Petri dishes with a fill depth of ~2 cm, were cooled to −45°C at 0.5°C/min followed by an isothermal hold for 180 min. Subsequently, primary drying was carried out at −45°C for 48 h at a pressure of 50 mTorr. The temperature was then increased to −30°C and held for 24 h, followed by holding at −10 and 0°C for 12 h each. The heating rate was 0.1°C/min. Subsequently, secondary drying was carried out at 25°C for 36 h. Sucrose was co-lyophilized with either sorbitol or PVP using the same protocol. The additive concentration in the final lyophile was 2.5% w/w.

Differential Scanning Calorimetry (DSC)

A differential scanning calorimeter (MDSC 2920, TA instruments, New Castle, DE) equipped with a refrigerated cooling accessory was used. The instrument was calibrated with pure indium and tin. About 15–20 mg of sample was weighed in an aluminum pan, which was then crimped non-hermetically. Glass transition and crystallization onset temperatures were determined by heating the sample, under nitrogen purge, from 25 to 120°C at 10°C/min.

X-ray Powder Diffractometry

About 100 mg of sample was filled in a copper holder and exposed to Cu Kα radiation (45 kV×40 mA) in a wide-angle X-ray diffractometer (Model D5005, Bruker, Madison, WI, USA). The instrument was operated in the step-scan mode, in increments of 0.05°2θ. The angular range was 5–40°2θ, and counts were accumulated for 1 s at each step. The data collection and analyses were performed with commercially available software (JADE, version 7, Materials Data Inc., Livermore, CA, USA). X-ray diffractometry was used to confirm that the samples prepared by lyophilization were amorphous.

Karl Fischer Titrimetry (KFT)

The water content was determined coulometrically using a Karl Fischer titrimeter (Model CA-05 Moisture Meter, Mitsubishi Chemical Corp, Kushima, Japan). Accurately weighed samples were directly added to the Karl Fischer cell and the water content was determined.

Dielectric Relaxation Spectroscopy (DRS)

Molecular mobility in the amorphous samples was measured using a dielectric relaxation spectrometer

(Novocontrol Alpha Analyzer, Novocontrol Technologies, Germany). The sample (~400 mg) was packed tightly between two copper-coated brass electrodes (20 mm diameter) enclosed by a PTFE spacer. The electrodes, in parallel plate configuration, were screwed securely to ensure intimate contact with the sample and to minimize air gaps. The PTFE spacer (thickness: 2.1 mm; area: 59.69 mm^2; capacity: 0.518 picoFarad) was used to contain the powder sample uniformly in the region between the parallel electrode plates. The capacitance of the PTFE spacer ring, as well as the estimated edge capacitance effects caused by the 20 mm diameter plates, were calculated and corrected for by the Novocontrol software. The electrodes were heated to the desired temperature at 20°C/min using a Novotherm® temperature controller. Instrument operations were controlled using WinDETA®, which allowed experiments to be carried out as a function of frequency at a fixed temperature (frequency sweep) or as a function of temperature at a fixed frequency (isochronal). The frequency range employed was 10^{-2} to 10^7 Hz for most experiments, and the total time taken for each measurement in this frequency range was ~35 min. α-relaxations were observed at temperatures (5° increments) ranging from 75 to 90°C for sucrose and sucrose-sorbitol systems and from 85 to 100°C for sucrose-PVP system. In order to avoid the risk of crystallization, the frequency range used for amorphous sucrose at 85 and 90°C and for sucrose-sorbitol system at 75 and 80°C was 10^{-1} to 10^7 Hz so that the experiments lasted ~15 min. For the same reason, the frequency range used for sucrose-sorbitol system at 85 and 90°C was 10^2–10^7 Hz, and the duration of the experiments was <5 min. At the end of the frequency sweep experiments, the samples were confirmed to be amorphous by X-ray diffractometry. For isochronal (temperature sweep) experiments, samples were heated to the desired temperature at 20°C/min, and measurements were made at 10°C intervals at a frequency of 1 kHz. The instrument was validated by measuring relative permittivity and dielectric loss of fused quartz at various temperatures and comparing with the reported values. Sample handling was carried out at room temperature in inert nitrogen atmosphere at <3% RH. The water content in all the lyophiles was consistently <0.5% w/w. After the experiments, the water content and the glass transition temperature were determined by KFT and DSC, respectively, and were found to be unaltered.

Analysis of Dielectric Relaxation Spectroscopy Data

The change in capacitance and conductance of the sample caused by dipole reorientation was measured, and subsequently the complex permittivity was calculated using these measured values and sample geometry. The complex dielectric function, $\varepsilon^*(\omega)$, described in Eq. 1 below, consists of the real part, $\varepsilon'(\omega)$, which gives the amplitude in-phase with the external field. $\varepsilon'(\omega)$ is called the dielectric permittivity and represents the energy stored in the dielectric material. The imaginary part $\varepsilon''(\omega)$ gives the amplitude out of phase with the external field by 90°. $\varepsilon''(\omega)$ is called the dielectric loss and represents the loss in energy when the external electric field passes through the dielectric material.

$$\varepsilon^*(\omega) = \varepsilon'(\omega) - \varepsilon''(\omega) \tag{1}$$

The maximum relaxation time (τ_{max}) is given by Eq. 2:

$$\tau_{max} = [2\pi f_{max}]^{-1} \tag{2}$$

where f_{max} is the frequency corresponding to maximum dielectric loss.

The basic model function describing a dielectric relaxation process is the Debye function shown in Eq. 3:

$$\varepsilon^*(\omega) = \varepsilon_\infty + \frac{\Delta\varepsilon}{1 + i\omega\tau} \tag{3}$$

τ is the relaxation time, and $\Delta\varepsilon$ is the dielectric strength or intensity given by $(\varepsilon_s - \varepsilon_\infty)$, where ε_s is the static permittivity or the low frequency limit $(\omega \to 0)$ of $\varepsilon'(\omega)$, and ε_∞ is the high frequency limit $(\omega \to \infty)$ of $\varepsilon'(\omega)$. According to the Debye model, the peak in the dielectric loss *versus* frequency profile is symmetric with a constant full width at half maximum value of 1.14 decade. The peak width is a direct measure of the distribution of relaxation times. In most cases, the peaks of dielectric relaxations are much broader and also asymmetric. The symmetric and asymmetric broadening of relaxation peaks can be described by the Havriliak-Negami function as in Eq. 4:

$$\varepsilon^*(\omega) = \varepsilon_\infty + \frac{\Delta\varepsilon}{\left(1 + (i\omega\tau)^{\beta_{HN}}\right)^{\gamma_{HN}}} + \frac{\sigma_0}{i\varepsilon_s\omega} \tag{4}$$

where β_{HN} is a parameter describing symmetric peak broadening with $0 < \beta \leq 1$, γ_{HN} is the asymmetric broadening parameter with $0 < \gamma \leq 1$, and σ_0 is the dc conductivity. The above equation also accounts for the dc conductivity typically observed at lower frequencies.

Fitting the relaxation profiles with the Havriliak-Negami equation was carried out using WinFIT® software.

As described later, we observed two secondary relaxations in sucrose, and the relaxation profiles were incompletely resolved with considerable overlapping. In such cases, it is a common practice to fit the relaxations simultaneously as has

been reported for trehalose and sucrose (20,37). Thus, we used two Havriliak-Negami functions to simultaneously fit the two β-relaxations (Eq. 5 below):

$$\varepsilon^*(\omega) = \sum_{i=1}^{2}\left[\varepsilon_{\infty i} + \frac{\Delta\varepsilon_i}{\left(1+(i\omega\tau_i)^{\beta_i}\right)^{\gamma_i}}\right] + \frac{\sigma_0}{i\varepsilon_s\omega} \quad (5)$$

For the β-relaxations, best fits were obtained with $\gamma = 0.8$, and the relaxation parameters τ and β were obtained from the profiles at different temperatures. β-relaxation times *versus* temperature data were fitted using Arrhenius equation, as in Eq. 6, wherever applicable:

$$\frac{1}{\tau} = A\exp\left[\frac{-E_a}{RT}\right] \quad (6)$$

where A is a pre-exponential factor, E_a is the activation energy, and R is the universal gas constant.

For α-relaxation, relaxation time τ as well as the parameters β and γ were obtained from the fitted profiles at different temperatures. The temperature dependence of relaxation time was fitted using the Vogel-Tammann-Fulcher (VTF) equation described in Eq. 7:

$$\ln(\tau) = \frac{DT_0}{T - T_0} + \ln(\tau_0) \quad (7)$$

where τ is the mean relaxation time, T is the temperature, τ_0 is the relaxation time at temperature T_0 and was fixed at 10^{-12} s, and D is the "strength" parameter reflecting the kinetic fragility of the system. Fragile glass formers typically have D-values <10, while strong glass formers are usually characterized by D-values >100. Thus, smaller D-values indicate increased fragility.

RESULTS AND DISCUSSION

Baseline Characterization

The model systems used were sucrose (no additives; control) and sucrose co-lyophilized with either PVP or sorbitol. The water content in all the lyophiles was consistently <0.5% w/w. The presence of additives (2.5% w/w) did not change the T_g (75±1°C) to a measurable extent. Taking the T_g of sucrose to be 75°C, the Fox equation predicts T_g values of ~73 and ~77°C for molecular dispersions of sucrose with 2.5% w/w of sorbitol and PVP respectively. It should be noted that for sucrose-PVP mixture, free volume additivity does not hold, and experimental T_g values are typically lower (39) than those predicted assuming ideal mixing (e.g., Gordon-Taylor or Fox equation).

α-Relaxations and Crystallization

As discussed earlier, the crystallization of amorphous sucrose is likely to be inhibited by PVP, attributable to inhibition of molecular motions. We also expect that sorbitol, at a concentration of 2.5% w/w, would facilitate sucrose crystallization by increasing global mobility. In order to test these hypotheses, both the glass transition and crystallization behavior were investigated by dielectric spectroscopy.

DSC measures glass transition as a change in heat capacity, and the glass transition temperatures measured by DSC were identical for all the systems. On the other hand, DRS probes the system at the molecular level by measuring dipolar reorientations in response to the electric field. We hypothesize that the latter technique, measuring the dielectric loss as a function of temperature, would be more responsive to α-relaxations. Thus, we expect to find differences in the onset temperature of α-relaxations (glass transition) as the glassy samples are heated through T_g. The model systems were subjected to a temperature sweep at a fixed frequency of 1 kHz in order to compare the glass transition and crystallization behavior. At this frequency, changes in the dielectric loss corresponding to α-relaxation associated with glass transition and crystallization were most prominent. It is clear from Fig. 1 that the onset and peak temperatures for both α-relaxation corresponding to glass transition and dielectric relaxation associated with crystallization are different in the three systems. The results are summarized in Table I. Compared to sucrose, the α-relaxation peak onset temperature was lower for the sucrose-sorbitol and higher for the sucrose-PVP system. This indicated higher mobility in sucrose-sorbitol system, while the α-relaxations were inhibited in the sucrose-PVP dispersion. A similar trend was observed in the crystallization of amorphous sucrose. At the end of the isochronal experiments, all the samples were confirmed to be crystalline by XRD. Crystallization onset, as indicated by an increase in dielectric loss corresponding to relaxation associated with crystallization, was at a higher temperature in presence of PVP and at a lower temperature for the sucrose-sorbitol system (Fig. 1). Crystallization onset temperatures measured by DSC exhibited a similar trend (Fig. 2). Thus, α-relaxations, or the global mobility, determined by dielectric spectroscopy, correlated with crystallization behavior, although the calorimetric glass transition temperatures were not significantly different.

Temperature Dependence of α-Relaxation Times

The temperature dependence of α-relaxation times was next investigated. As the experimental temperature increased, the

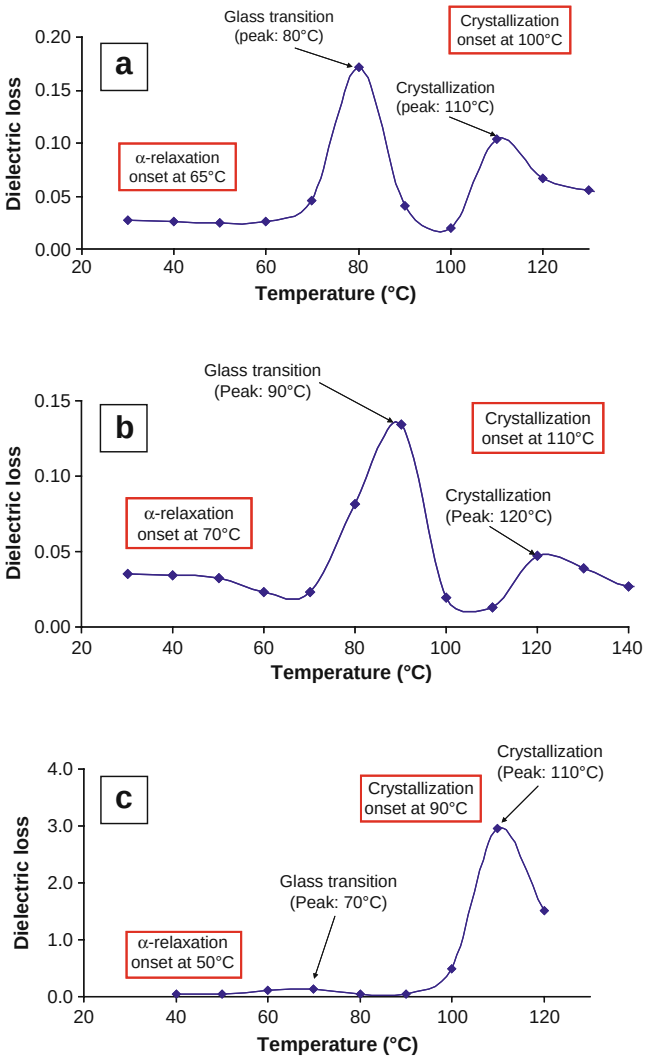

Fig. 1 Plots of dielectric loss *versus* temperature in (**a**) sucrose, (**b**) sucrose co-lyophilized with PVP (2.5% w/w) and (**c**) sucrose co-lyophilized with sorbitol (2.5% w/w). Dielectric relaxation associated with glass transition and crystallization has been shown. The experiments were carried out at a frequency of 1 kHz. Lines have been drawn to assist in visualizing the trends.

α-relaxation peak in amorphous sucrose shifted to higher frequency, indicating an increase in the relaxation rates (Fig. 3). Similar observations were made for the sucrose-PVP and sucrose-sorbitol systems. The α-relaxation peaks were modeled using the Havriliak-Negami equation, and the relaxation parameters were obtained. The symmetric broadening parameter, β_{HN}, was found to be similar for all the model systems (~0.6) and showed negligible change with temperature. The asymmetry broadening parameter (γ_{HN}) was also found to be almost constant (~0.7). The negligible change of these parameters with temperature is expected, since α-relaxations become more homogeneous above the T_g, and dynamic heterogeneity is less sensitive to temperature. However, dynamic heterogeneity between the systems will be discussed later in terms of the more sensitive fragility parameter. The relaxation times were plotted against temperature for all the systems. Figure 4 shows the relaxation times of amorphous sucrose and sucrose-sorbitol systems at temperatures ranging from 75 to 90°C. α-relaxations were observed only at ≥85°C in the sucrose-PVP system for the experimental frequency range used. The relaxation time *versus* temperature plots were fitted to the VTF equation. It is evident that compared to sucrose, the relaxation times were longer for sucrose-PVP and shorter for sucrose-sorbitol at all the temperatures studied. This clearly shows the inhibition of cooperative motions by PVP and increase in the mobility brought about by sorbitol. Table I lists the average α-relaxation times at the respective calorimetric T_g of the model systems. α-relaxation time for amorphous sucrose at T_g was determined to be ~4.2 s, which is in agreement with the literature value of 3 s (2). This confirms that the generally accepted relaxation time of 100 s at calorimetric T_g is not universally valid. The same argument holds true for the sucrose-sorbitol as well as the sucrose-PVP systems, which were characterized by relaxation times of ~0.2 and ~$2.4*10^3$ s, respectively, at T_g. For the sucrose-PVP system, the corresponding value was calculated using the fitted VTF equation. The observed differences in relaxation times are especially remarkable considering that the glass transition temperatures determined by DSC were identical.

Kinetic Fragility of the Model Glass-Formers

Attempts have been made to explain crystallization from the supercooled liquid state in terms of fragility (40). The more fragile the system, the larger the deviation of viscosity or relaxation time from Arrhenius behavior. It is well known that at low degree of supercooling, i.e., near the melting point of a crystal, crystal growth rate initially increases and is limited by the thermodynamic driving force for crystallization. However, if the liquid is further cooled, the viscosity gradually increases and the crystal growth rate is then determined by molecular mobility or the self-diffusion coefficient of the liquid (41). The self-diffusion coefficient has been found to scale inversely with viscosity (η^{-1}). However, it has been argued that the more fragile a material, the more decoupled is the self-diffusion coefficient, and hence crystal growth near T_g, from an inverse scaling with the viscosity (40). An increase in fragility results in an increase non-exponentiality in the relaxation rates near T_g and is likely to have a strong influence on the crystal growth kinetics. We therefore compared the VTF strength parameter (D) of the three systems (Table I). The D-value of ~5.9 for amorphous sucrose is in agreement with the reported value of 7.3 (6) and is indicative of a very fragile glass former. While the influence of additives on T_0

Table I Global and Local Mobility Parameters of Sucrose and Sucrose Co-lyophilized with PVP or Sorbitol

	Sucrose	Sucrose + 2.5% w/w PVP	Sucrose + 2.5% w/w Sorbitol
α-relaxation onset (°C)	65 ± 1	70 ± 1	50 ± 1
Crystallization onset (°C)	100 ± 1	110 ± 2	90 ± 1
α-relaxation time at T_g (seconds)[a]	4.2[c]	$2.4 \cdot 10^{3}$ [b]	$2.3 \cdot 10^{-1}$[c]
β_1-relaxation time at T_g (seconds)[a]	$3.7 \cdot 10^{-5}$ [b]	$2.2 \cdot 10^{-7}$ [b,e]	$8.3 \cdot 10^{-6}$ [b]
β_2-relaxation time at T_g (seconds)[a]	$5.7 \cdot 10^{-9}$ [b]	$8.5 \cdot 10^{-11}$ [b,e]	$2.8 \cdot 10^{-10}$ [b]
Independent relaxation time (seconds)[a]	$2.9 \cdot 10^{-6}$ [b]	$6.9 \cdot 10^{-5}$ [b]	$6.8 \cdot 10^{-7}$ [b]
T_0 (K)	289 ± 2	293 ± 2	301 ± 3
D	5.9 ± 0.3	6.5 ± 0.2[d]	4.1 ± 0.2[d]
$\tau_{\beta 1}$ at (T_g-50) (seconds)	$2.3 \cdot 10^{-3} \pm 3.4 \cdot 10^{-4}$	$1.1 \cdot 10^{-2} \pm 3.3 \cdot 10^{-3}$	$2.5 \cdot 10^{-3} \pm 4.6 \cdot 10^{-4}$
β_1-relaxation activation energy (kJ/mol)	60 ± 2	40 ± 1 to 232 ± 2	83 ± 1
$\tau_{\beta 2}$ at (T_g-50) (seconds)	$3.0 \cdot 10^{-7} \pm 2.3 \cdot 10^{-8}$	$2.0 \cdot 10^{-7} \pm 7.1 \cdot 10^{-8}$	$3.2 \cdot 10^{-7} \pm 3.9 \cdot 10^{-8}$
β_2-relaxation activation energy (kJ/mol)	63 ± 2	11 ± 1 to 189 ± 1	132 ± 3
Model for β_1- and β_2-relaxations	Arrhenius	Non-Arrhenius	Arrhenius

[a] Mean values

[b] Calculated values

[c] Experimentally measured values (standard deviations given in Fig. 4)

[d] Significantly different from sucrose ($\alpha = 0.05$; two-tailed test)

[e] Since the system exhibited non-Arrhenius behavior, the calculation was based on the relaxation times at 50 and 60°C only.

was rather small, the D-values were significantly different (Table I). The sucrose-PVP system, having a decreased global mobility and crystallization tendency compared to amorphous sucrose, was found to have a higher D-value. On the other hand, the sucrose-sorbitol system, having an increased global mobility and crystallization tendency compared to amorphous sucrose, was characterized by a lower D-value or higher fragility. This suggests that the three systems are characterized by different extents of heterogeneity in relaxation dynamics near T_g. Their marked differences in global mobility as well as dynamic heterogeneity are probably responsible for the differences in crystallization behavior.

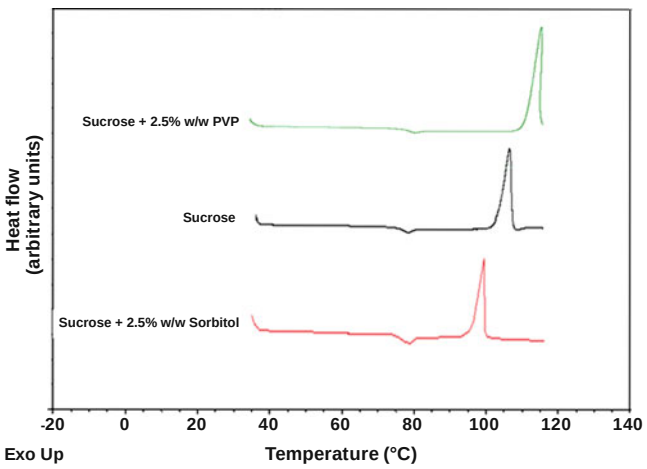

Fig. 2 DSC heating curves of sucrose lyophilized alone or co-lyophilized with either PVP or sorbitol. While the additive did not have a pronounced effect on the glass transition, the onset of crystallization occurred at a higher temperature in the presence of PVP and at lower temperature in the presence of sorbitol.

Local Mobility in the Model Systems

Our next objective was to investigate secondary relaxations below T_g in the model systems. Figure 5 shows the relaxation profile of glassy sucrose at 50°C. At this temperature, which is 25° below the T_g, relaxation peaks correspond to the local motions, since the cooperative α-relaxations are minimal. As is evident from the figure, the low frequency region is dominated by dc conductivity, but

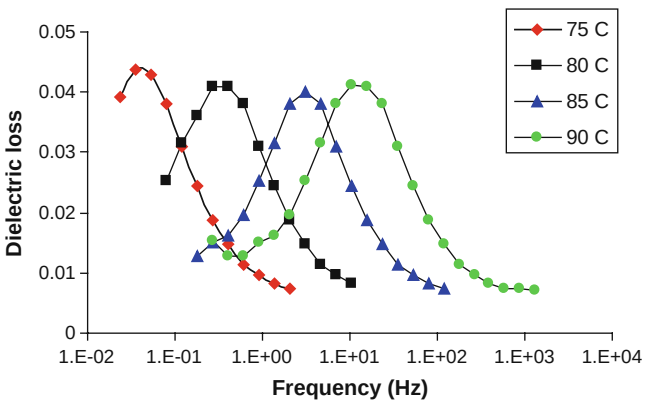

Fig. 3 Plot of dielectric loss as a function of frequency for amorphous sucrose at 75, 80, 85 and 90°C. The data were fitted to the Havriliak-Negami equation.

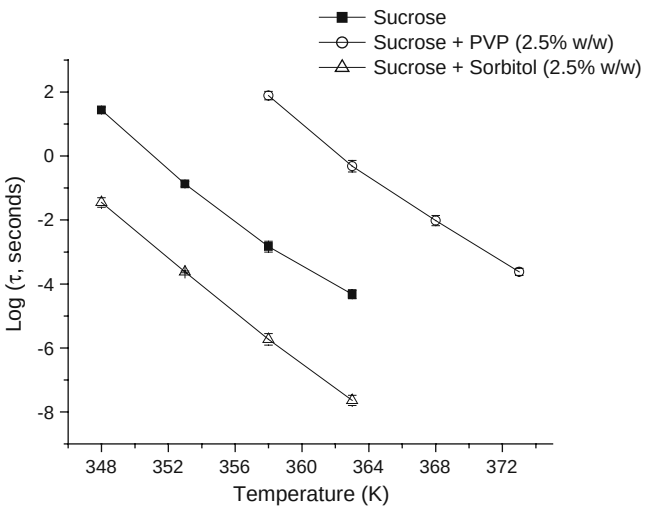

Fig. 4 Temperature dependence of relaxation times of amorphous sucrose and sucrose co-lyophilized with PVP or sorbitol. Lines are fits to the VTF equation. *Error bars* (standard deviations; $n \geq 3$), when invisible, are smaller than the size of the symbols. χ^2 values for VTF fits were 0.040, 0.015 and 0.051, respectively, for sucrose, sucrose-PVP and sucrose-sorbitol systems.

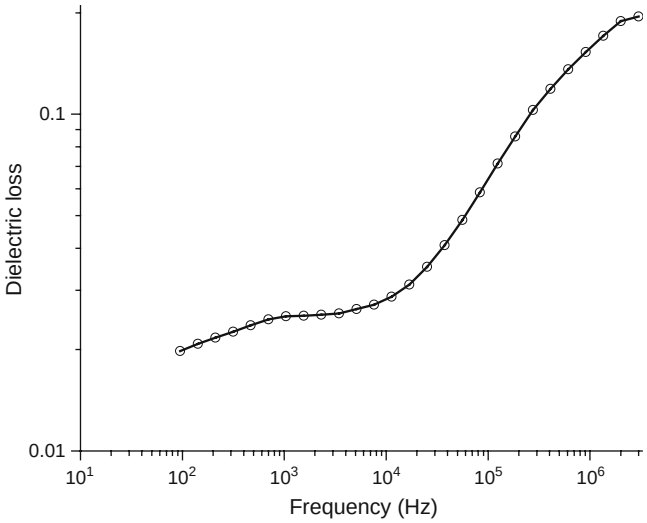

Fig. 6 Simultaneous fitting of β_1- and β_2-relaxations in amorphous sucrose at 50°C using two Havriliak-Negami functions. $\chi^2 = 0.0027$; $\tau_{\beta_1} = 2.06*10^{-4} \pm 3.15*10^{-6}$s, $\tau_{\beta_2} = 2.65*10^{-8} \pm 1.67*10^{-10}$s, $\beta_{HN}(\beta_1) = 0.39 \pm 0.00$, $\beta_{HN}(\beta_2) = 0.43 \pm 0.01$. Asymmetry parameter γ was fixed at 0.8.

two unresolved β-relaxation peaks (secondary relaxation) appear at higher frequencies, similar to a recent report as discussed earlier (37). Data reproducibility has been shown by overlay of three representative data sets (Fig. 5; inset). The two unresolved β-relaxations were simultaneously fitted using the Havriliak-Negami equation. Figure 6 is a representative fit for amorphous sucrose at 50°C showing the fit parameters. For β-relaxations, best fits were obtained with the asymmetric broadening parameter (γ_{HN}) fixed at 0.8. We designate the slower β-relaxation, i.e., the one appearing at lower frequency as β_1 and the faster one as β_2. The dielectric loss, and hence dielectric strength (a measure of relaxation strength), of the β_2-relaxation was higher than that of the β_1-relaxation. This is in agreement with the literature reports showing a higher dielectric strength for the faster of the two β-relaxations in hydrogen-bonded glasses (36,37). However, the dielectric strength was essentially unchanged in the temperature range (30–50°C for β_1- and 30–70°C for β_2-relaxations) studied (data not shown). The width parameter (β_{HN}) was higher for the β_2-relaxation, implying that the faster β-relaxation is dynamically more homogeneous.

The sucrose-sorbitol and sucrose-PVP systems were also characterized by two β-relaxations which shifted to higher

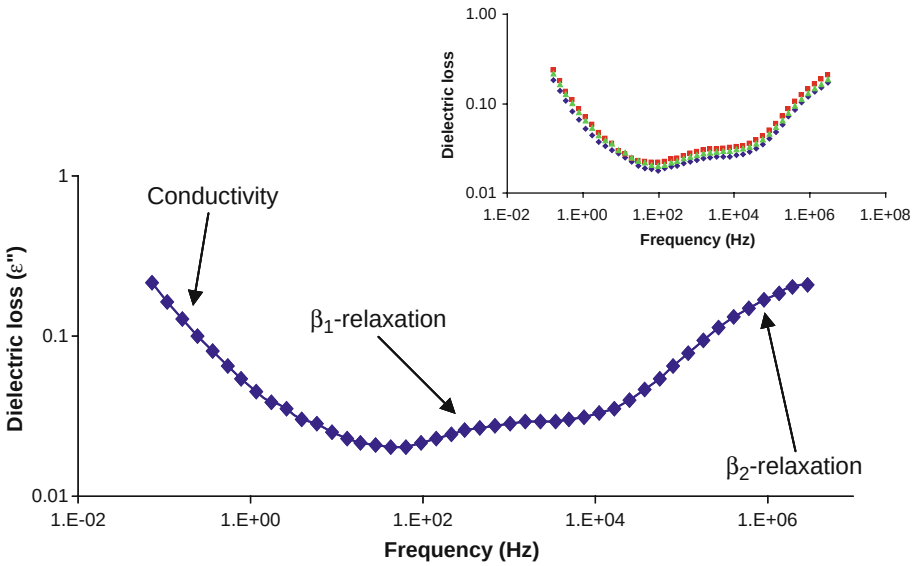

Fig. 5 Dielectric relaxation profiles of amorphous sucrose at 50°C (T_g-25). Contributions from conductivity and the two β-relaxations have been shown. The inset is the overlay of three dielectric relaxation profiles at 50°C, showing experimental reproducibility.

frequencies with an increase in temperature. The β_1- and β_2-relaxation times for the three systems have been plotted as a function of temperature (Figs. 7 and 8). While the temperature dependence of β_1- and β_2-relaxation times for the sucrose and sucrose-sorbitol systems could be fitted using the Arrhenius equation, the corresponding plots for sucrose-PVP system showed significant deviation (Table I contains the activation energies). The activation energies of both the β-relaxations in sucrose are approximately the same. The activation energy of the overall β-relaxation in sucrose, E_β, calculated from the empirical equation (42,43), $E_\beta = (24 \pm 3)RT_g$, where R is the gas constant, ranges from 60.8 to 78.1 kJ/mol. Our experimentally determined values of the β_1- (60 kJ/mol) and β_2-relaxations (63 kJ/mol) reported in Table I are in agreement with these calculated values. Our values are also close to the literature values for β-relaxation in other sugars (20,44–46). Interestingly, Kaminski *et al.* reported the activation energy of β_1- and β_2-relaxations (designated "β-" and "γ-" respectively by the authors) in sucrose to be 96 and 52 kJ/mol, respectively (37). Our results show good agreement in the activation energy value of β_2- but not β_1-relaxations. The observed differences in the activation energies could be attributed to the method of preparation of amorphous sucrose. We prepared amorphous sucrose by lyophilization, while Kaminski *et al.* (37) used melt-quenching. Amorphous phases prepared by different methods have been documented to exhibit different properties (47) attributable to differences in their thermal histories. This effect is expected to be pronounced on the Johari-Goldstein relaxations, which are strongly influenced by thermal history (21,48,49). Also, as pointed out earlier, since Kaminski *et al.* prepared amorphous sucrose by melt quenching, the possibility of sucrose decomposition cannot be ruled out. Contrary to our findings as well as literature

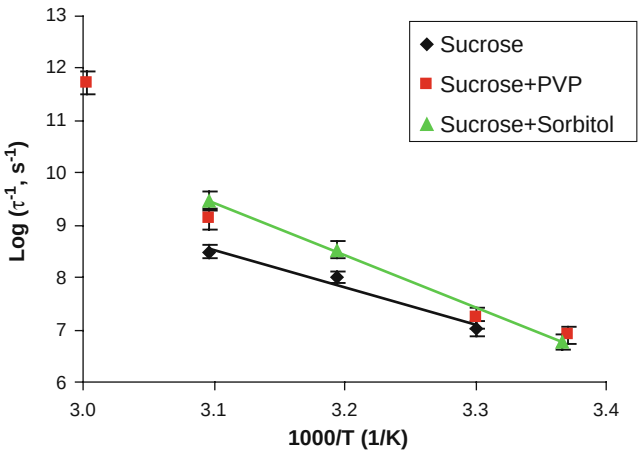

Fig. 7 Temperature dependence (Arrhenius) of β_1-relaxation time in sucrose and sucrose co-lyophilized with sorbitol. The sucrose-PVP system exhibited non-Arrhenius behavior. The additive concentration was 2.5% w/w.

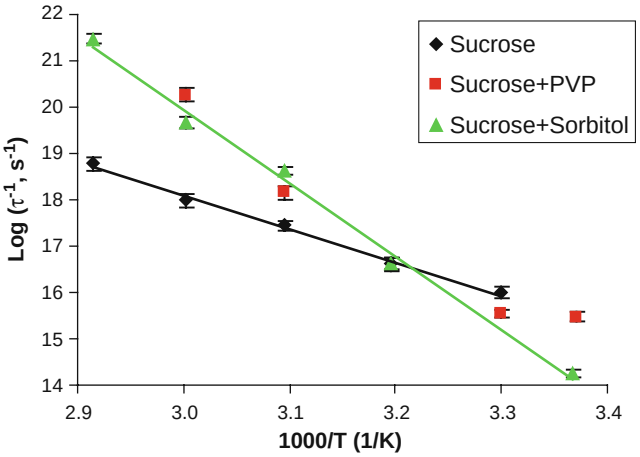

Fig. 8 Temperature dependence (Arrhenius) of β_2-relaxation time in sucrose and sucrose co-lyophilized with sorbitol. The sucrose-PVP system exhibited non-Arrhenius behavior. The additive concentration was 2.5% w/w.

reports (2), these authors did not observe an α-relaxation peak at the calorimetric T_g in amorphous sucrose. Thus, it appears that the samples investigated by Kaminski *et al.* were "different" from the lyophilized sucrose used by us.

The presence of sorbitol resulted in an increase in the activation energy of both the β-relaxations in sucrose, suggesting inhibition of local motions in sucrose by sorbitol. The increase in the activation energy of the β_2-relaxation was more than that of the β_1-relaxation. Inhibition of local motions of an organic glass by a small molecule additive having a lower T_g, while counterintuitive, is well documented. Although glycerol has a lower T_g than trehalose and causes an increase in the global mobility, it has an anti-plasticizing effect on trehalose local motions (50,51). An increase in the water content caused an increase in the activation energy of β-relaxations in poly(vinyl pyrrolidone) (52). The different extents of inhibition of the two β-relaxations are probably attributable to differences in the origins of these local motions. Glassy sorbitol has been reported to exhibit a J-G type β-relaxation (49) with an activation energy of 75 kJ/mol (53) and is also likely to contribute to the local motions of sucrose, although the extent of contribution could be expected to be small due to the low sorbitol concentration. Both sucrose and sorbitol are heavily hydrogen-bonded systems, and thus hydrogen bonding is very likely to play a major role in influencing the local mobility. The fact that increase in the activation energy of β_2-relaxation was more than that of β_1-relaxation, in sucrose-sorbitol solid dispersions, suggests that sucrose-sorbitol interactions have a much greater effect on the faster secondary relaxation of sucrose. These findings could have great implications in stabilization of solid dispersions. For example, if the local motions of an active pharmaceutical ingredient (API) are coupled to its physical stability, then

the inclusion of an amorphous excipient with a lower T_g in the solid dispersion matrix could be an effective strategy to stabilize the API.

The activation energy of β-relaxations in PVP has been reported to range from ~37 (52) to ~46 kJ/mol (54). The significant curvature in the temperature dependence of both the β_1- and β_2-relaxation times in the sucrose-PVP system could result from the contributions of PVP local motions. Although the PVP concentration was only 2.5% w/w, the effect may be attributed to the much high molar concentration of the monomers. Since there was no phase separation (single T_g), the local motions are most likely a combination of those of sucrose and the PVP monomers. The β_1- and β_2-relaxation times were measured at four temperatures below T_g, and the relaxation times at the two lowest temperatures yielded the lowest activation energy and at the two highest temperatures yielded the highest activation energy. These provided a rough estimate of the change in activation energy with temperature (Table I). The activation energy increased with temperature, suggesting inhibition of local motions at higher temperatures. Sucrose has been shown to be extensively hydrogen bonded to PVP (39,55). Thus, hydrogen bonding could be speculated to play a major role in the temperature-dependent inhibition of local mobility. Polymers such as PVP are very often used for preparing solid dispersions of organic small molecule APIs, and it is important to be aware of such effects in light of the potential significance of local motions on API stability.

The fact that glassy sucrose shows two secondary relaxations, which are affected by additives, highlights the importance of molecular motions below the T_g. As discussed earlier, the Kauzmann temperature (T_g-50) has long been accepted in the pharmaceutical community as the temperature of "zero mobility." However, the β-relaxations persist well below T_g, and thus there are pronounced local motions even at (T_g-50), as shown in Table I. These extrapolated values were obtained assuming Arrhenius behavior. Thus, it is important to rule out the coupling of local mobility with instability before assuming the negligible role of molecular mobility upon storage far below T_g.

Correlation Between α- and β-Relaxations

Two secondary relaxations have been observed in several monosaccharides and disaccharides (20,44). With one exception (20), the slower β-relaxation was generally argued to be the Johari-Goldstein relaxation (44). Identification of the JG relaxation is important, since it is the only kind of local motion that has been argued to be the precursor to glass transition and hence is likely to be important for the stability of small molecules.

According to the coupling model of Ngai, the molecular dynamics of supercooled liquids involve three time regimes: short, intermediate, and long. The short-time regime is described by vibrational motions and an exponential decay of the relaxation time. The intermediate-time regime is characterized by non-cooperative independent relaxations, also called "primitive" α-relaxations, with gradually increasing cooperativity. The long-time regime consists of the slower cooperative α-relaxations, explained by the Kohlrausch-Williams-Watts (KWW) stretched exponential function, $\exp\left(-\frac{t}{\tau}\right)^{\beta_{KWW}}$, where β_{KWW} is a measure of the deviation from exponential decay. The independent relaxations are related to the cooperative α-relaxations by a crossover time, τ_c, which is independent of temperature. The independent relaxations take place at times less than τ_c, whereas at times longer than τ_c, these are transformed into the cooperative slower α-relaxations as a result of intermolecular interactions. The value of τ_c was determined to be about 2 picoseconds for glass-forming polymers by quasielastic neutron scattering (56,57) and has been argued to be also valid for small molecule organic glass formers (58). The independent relaxation time, τ_0, could be calculated from empirical correlations with the α-relaxation time, τ_α, at T_g using Eq. 8 (58):

$$\tau_0 = \tau_\alpha^{\beta_{KWW}} * \tau_c^{(1-\beta_{KWW})} \tag{8}$$

Interestingly, JG relaxation times have been found to be close to calculated values of non-cooperative independent relaxation times in many glass formers and thus are implicated in heralding the cooperative molecular motions. Although Kaminski *et al.* suggested the JG nature of the slower secondary relaxation in sucrose, their arguments were based on indirect observations due to absence of the α-relaxation peak at T_g (37). We have calculated the independent relaxation times for our systems at T_g from the experimentally obtained α-relaxation parameters and compared them with the respective β-relaxation times at T_g.

The α-relaxation time distribution parameter from the KWW equation, β_{KWW}, was calculated from the Havriliak-Negami peak width parameters β_{HN} and γ_{HN} according to the empirical Eq. 9 (59):

$$\beta_{KWW} = (\beta_{HN}\gamma_{HN})^{\frac{1}{1.23}} \tag{9}$$

For α-relaxation at T_g, the symmetric broadening parameter (β_{HN}) was taken to be 0.6 (±0.004) for all the model systems, while the asymmetry broadening parameter (γ_{HN}) was 0.7 (±0.006). Although α-relaxation was not detected for sucrose-PVP system at T_g, the peak width parameters were not significantly different from the remaining systems at other temperatures and also showed negligible change with temperature. Using the above values, β_{KWW} was calculated to be 0.5. The β_1- and β_2-relaxation times at T_g were calculated using the

Arrhenius equation. The calculated values of independent relaxation time, τ_0, have been listed along with the β_1- and β_2-relaxation times at T_g in Table I. Compared to β_2-, the β_1-relaxation times at T_g are much closer to the τ_0 values, suggesting that the β_1-relaxation is of the Johari-Goldstein type and is correlated with the cooperative α-relaxations. The β_2-relaxation is probably the result of hydrogen bonding interactions. This argument is further supported by the report where the role of hydrogen bonding in molecular dynamics of dipropylene glycol (DPG) and dipropylene glycol dimethyl ether (DPGDME) was investigated (36). The two compounds have similar structure, but the latter is devoid of hydrogen bonding. While two β-relaxations were observed in DPG, only one was observed in DPGDME. The only β-relaxation in DPGDME as well as the slower β-relaxation in DPG was identified to be the JG relaxation based on the observed correlation with α-relaxations. The faster β-relaxation in DPG was concluded to result from hydrogen bonding interactions. Thus, hydrogen-bonded molecules are likely to exhibit multiple relaxations, the slower of which is likely to be the JG relaxation.

Significance

In a solid dosage form containing an amorphous API, the method of preparation, the excipients in the dosage form and the storage conditions (temperature and water vapor pressure) can influence its mobility, and thereby the stability. While differential scanning calorimetry is extensively used to characterize amorphous pharmaceuticals, the technique may grossly underestimate mobility. This was evident when the α-relaxation onset temperatures, determined by DRS, were observed to be substantially different from the calorimetric T_g values. Moreover, the plasticizing effect of sorbitol and the anti-plasticizing effect of PVP on the global mobility were revealed by DRS, while the calorimetric glass transition temperatures were unaffected by the additives. The excipient effects on global mobility cannot be a predictor of the effects on local mobility. Sorbitol, by inhibiting local motions, increased the activation energy for β-relaxations, while PVP exhibited a temperature-dependent inhibition of local motions. In systems exhibiting multiple secondary relaxations, it is instructive to identify the specific relaxation that is coupled to global mobility. Such information would be useful when the mobility is coupled to stability.

CONCLUSIONS

Conventionally, calorimetric T_g is used as a marker of molecular mobility and forms the basis for the selection of additives as well as their levels in solid dispersions. Our work has highlighted the deficiency of this approach and the need to use more discriminatory methods like dielectric spectroscopy. We demonstrated how relatively low levels of additives could significantly affect molecular mobility in amorphous solid dispersions without changing the T_g. Global mobility as well as VTF strength parameter as a measure of kinetic fragility correlated very well with the crystallization tendency of the model systems. The significance of local mobility in amorphous pharmaceuticals either as a precursor to global mobility or with a direct role in crystallization was discussed. The slower β-relaxation in sucrose solid dispersions was found to mimic the behavior of Johari-Goldstein relaxations and hence was argued to be correlated with the α-relaxation. Lastly, the importance of local mobility implications of commonly used solid dispersion additives was emphasized in light of the local motions in sucrose-additive dispersions. While PVP caused a change in the temperature dependence of both the β-relaxation times, sorbitol inhibited both the local motions, indicating a potential stabilization strategy in systems where local mobility is coupled to physical stability.

ACKNOWLEDGMENTS

We thank Brad Givot (3M, St. Paul, MN) for all his help, support and insightful comments during the course of the project, and 3M (St. Paul, MN) for providing us generous access to the dielectric spectrometer. Sunny Bhardwaj is thanked for his comments.

REFERENCES

1. Pouton CW. Formulation of poorly water-soluble drugs for oral administration: physicochemical and physiological issues and the lipid formulation classification system. Eur J Pharm Sci. 2006;29:278–87.
2. Bhugra C, Rambhatla S, Bakri A, Duddu SP, Miller DP, Pikal MJ, *et al.* Prediction of the onset of crystallization of amorphous sucrose below the calorimetric glass transition temperature from correlations with mobility. J Pharm Sci. 2007;96:1258–69.
3. Bhugra C, Shmeis RA, Krill SL, Pikal MJ. Predictions of onset of crystallization from experimental relaxation times I-Correlation of molecular mobility from temperatures above the glass transition to temperatures below the glass transition. Pharm Res. 2006;23:2277–90.
4. Bhugra C, Shmeis RA, Krill SL, Pikal MJ. Prediction of onset of crystallization from experimental relaxation times. II. Comparison between predicted and experimental onset times. J Pharm Sci. 2008;97:455–72.
5. Shamblin SL, Hancock BC, Pikal MJ. Coupling between chemical reactivity and structural relaxation in pharmaceutical glasses. Pharm Res. 2006;23:2254–68.
6. Shamblin SL, Tang X, Chang L, Hancock BC, Pikal MJ. Characterization of the time scales of molecular motion in pharmaceutically important glasses. J Phys Chem B. 1999;103:4113–21.
7. Craig DQM, Royall PG, Kett VL, Hopton ML. The relevance of the amorphous state to pharmaceutical dosage

forms: glassy drugs and freeze-dried systems. Int J Pharm. 1999;179:179–207.
8. Yu L. Amorphous pharmaceutical solids: preparation, characterization and stabilization. Adv Drug Deliv Rev. 2001;48:27–42.
9. Kerc J, Srcic S. Thermal analysis of glassy pharmaceuticals. Thermochim Acta. 1995;248:81–95.
10. Hilden LR, Morris KR. Physics of amorphous solids. J Pharm Sci. 2001;93:3–12.
11. Vyazovkin S, Dranca I. Effect of physical aging on nucleation of amorphous indomethacin. J Phys Chem B. 2007;111:7283–7.
12. Yoshioka S, Miyazaki T, Aso Y. β-relaxation of insulin molecule in lyophilized formulations containing trehalose or dextran as a determinant of chemical reactivity. Pharm Res. 2006;23:961–6.
13. Yoshioka S, Miyazaki T, Aso Y, Kawanishi T. Significance of local mobility in aggregation of β-galactosidase lyophilized with trehalose, sucrose or stachyose. Pharm Res. 2007;24:1660–7.
14. Alie J, Menegotto J, Cardon P, Duplaa H, Caron A, Lacabanne C, *et al.* Dielectric study of the molecular mobility and the isothermal crystallization kinetics of an amorphous pharmaceutical drug substance. J Pharm Sci. 2004;93:218–33.
15. Hikima T, Adachi Y, Hanaya M, Oguni M. Determination of potentially homogeneous-nucleation-based crystallization in o-terphenyl and an interpretation of the nucleation-enhancement mechanism. Phys Rev B Condens Matter. 1995;52:3900–8.
16. Hikima T, Hanaya M, Oguni M. Discovery of a potentially homogeneous-nucleation-based crystallization around the glass transition temperature in salol. Solid State Commun. 1995;93:713–7.
17. Hikima T, Hanaya M, Oguni M. Microscopic observation of a peculiar crystallization in the glass transition region and β-process as potentially controlling the growth rate in triphenylethylene. J Mol Struct. 1999;479:245–50.
18. Hikima T, Okamoto N, Hanaya M, Oguni M. Calorimetric study of triphenylethene: observation of homogeneous-nucleation-based crystallization. J Chem Thermodyn. 1998;30:509–23.
19. Sixou B, Faivre A, David L, Vigier G. Intermolecular and intramolecular contributions to the relaxation process in sorbitol and maltitol. Mol Phys. 2001;99:1845–50.
20. Gusseme AD, Carpentier L, Willart JF, Descamps M. Molecular mobility in supercooled trehalose. J Phys Chem B. 2003;107:10879–86.
21. Johari GP. Intrinsic mobility of molecular glasses. J Chem Phys. 1973;58:1766–70.
22. Johari GP, Goldstein M. Viscous liquids and the glass transition. II. Secondary relaxations in glasses of rigid molecules. J Chem Phys. 1970:2372–2388.
23. Ngai KL. An extended coupling model description of the evolution of dynamics with time in supercooled liquids and ionic conductors. J Phys Condens Matter. 2003;15:S1107–25.
24. Hancock BC, Shamblin SL, Zografi G. Molecular mobility of amorphous pharmaceutical solids below their glass transition temperatures. Pharm Res. 1995;12:799–806.
25. Vyazovkin S, Dranca I. Probing beta relaxation in pharmaceutically relevant glasses by using DSC. Pharm Res. 2006;23:422–8.
26. Zeng XM, Martin GP, Marriott C. Effects of molecular weight of polyvinylpyrrolidone on the glass transition and crystallization of co-lyophilized sucrose. Int J Pharm. 2001;218:63–73.
27. Shamblin SL, Huang EY, Zografi G. The effects of co-lyophilized polymeric additives on the glass transition temperature and crystallization of amorphous sucrose. J Therm Anal. 1996;47:1567–79.
28. Shamblin SL, Zografi G. The effects of absrobed water on the properties of amorphous mixtures containing sucrose. Pharm Res. 1999;16:1119–24.
29. Johari GP, Kim S, Shanker RM. Dielectric studies of molecular motions in amorphous solid and ultraviscous acetaminophen. J Pharm Sci. 2005;94:2207–23.
30. Crowley KJ, Zografi G. The use of thermal methods for predicting glass-former fragility. Thermochim Acta. 2001;380:79–93.
31. Kremer F. Dielectric spectroscopy—yesterday, today and tomorrow. J Non-Cryst Solids. 2002;305:1–9.
32. Kremer F, Schonhals A, editors. Broadband dielectric spectroscopy. Berlin: Springer; 2003.
33. Craig DQM. Dielectric analysis of pharmaceutical systems. London: Taylor & Francis; 1995.
34. Hancock BC, Zografi G. Characteristics and significance of the amorphous state in pharmaceutical systems. J Pharm Sci. 1997;86:1–12.
35. Alig I, Braun D, Langendorf R, Voigt M, Wendorff JH. Simultaneous aging and crystallization processes within the glassy state of a low molecular weight substance. J Non-Cryst Solids. 1997;221:261–4.
36. Grzybowska K, Pawlus S, Mierzwa M, Paluch M, Ngai KL. Changes of relaxation dynamics of a hydrogen-bonded glass former after removal of the hydrogen bonds. J Chem Phys. 2006;125:144507/1–8.
37. Kaminski K, Kaminska E, Hensel-Bielowka E, Chelmecka E, Paluch M, Ziolo J, *et al.* Identification of the molecular motions responsible for the slower secondary (β) relaxation in sucrose. J Phys Chem B. 2008;112:7662–8.
38. Vanhal I, Blond G. Impact of melting conditions of sucrose on its glass transition temperature. J Agr Food Chem. 1999;47:4285–90.
39. Shamblin SL, Taylor LS, Zografi G. Mixing behavior of colyophilized binary systems. J Pharm Sci. 1998;87(6):694–701.
40. Ediger MD, Harrowell P, Yu L. Crystal growth kinetics exhibit a fragility-dependent decoupling from viscosity. J Chem Phys. 2008;128:034709/1–6.
41. Sun Y, Xi H, Ediger MD, Yu L. Diffusionless crystal growth from glass has precursor in equilibrium liquid. J Phys Chem B. 2008;112:661–4.
42. Kudlik A, Benkhof S, Blochowicz T, Tschirwitz C, Rossler E. The dielectric response of simple organic glass formers. J Mol Struct. 1999;479:201–18.
43. Ngai KL, Capaccioli S. Relation between the activation energy of the Johari-Goldstein β relaxation and T_g of glass formers. Phys Rev E. 2004;69:031501/1–5.
44. Kaminski K, Kaminska E, Paluch M, Ziolo J, Ngai KL. The true Johari-Goldstein β-relaxation of monosaccharides. J Phys Chem B. 2006;110:25045–9.
45. Noel TR, Ring SG, Whittam MA. Dielectric relaxations of small carbohydrate molecules in the liquid and glassy states. J Phys Chem. 1992;96:5662–7.
46. Noel TR, Parker R, Ring SG. Effect of molecular structure and water content on the dielectric relaxation behavior of amorphous low molecular weight carbohydrates above and below their glass transition. Carbohydr Res. 2000;329:839–45.
47. Surana R, Pyne A, Suryanarayanan R. Effect of preparation method on physical properties of amorphous trehalose. Pharm Res. 2004;21:1167–76.
48. Johari GP. Effect of annealing on the secondary relaxations in glasses. J Chem Phys. 1982;77:4619–26.
49. Ngai KL, Paluch M. Classification of secondary relaxation in glass-formers based on dynamic properties. J Chem Phys. 2004;120:857–73.
50. Cicerone MT, Soles CL. Fast dynamics and stabilization of proteins: binary glasses of trehalose and glycerol. Biophys J. 2004;86:3836–45.

51. Cicerone MT, Tellington A, Trost L, Sokolov A. Substantially improved stability of biological agents in dried form. BioProcess Int. 2003;1:36–47.
52. Duddu SP, Sokoloski TD. Dielectric analysis in the characterization of amorphous pharmaceutical solids. 1. Molecular mobility in poly(vinylpyrrolidone)-water systems in the glassy state. J Pharm Sci. 1995;84:773–6.
53. Nozaki R, Suzuki D, Ozawa S, Shiozaki Y. The α and the β relaxation processes in supercooled sorbitol. J Non-Cryst Solids. 1998;235–237:393–8.
54. Jain SK, Johari GP. Dielectric studies of molecular motions in the glassy states of pure and aqueous poly(vinylpyrrolidone). J Phys Chem. 1988;92:5851–4.
55. Taylor LS, Zografi G. Sugar-polymer hydrogen bond interactions in lyophilized amorphous mixtures. J Pharm Sci. 1998;87:1615–21.
56. Colmenero J, Arbe A, Alegria A. Crossover from Debye to non-Debye dynamical behavior of the α relaxation observed by quasielastic neutron scattering in a glass-forming polymer. Phys Rev Lett. 1993;71:2603–6.
57. Colmenero J, Arbe A, Alegria A. The dynamics of the α- and β-relaxations in glass-forming polymers studied by quasielastic neutron scattering and dielectric spectroscopy. J Non-Cryst Solids. 1994;172–174:126–37.
58. Ngai KL. Relation between some secondary relaxations and the α relaxations in glass-forming materials according to the coupling model. J Chem Phys. 1998;109:6982–94.
59. Alvarez F, Alegria A, Colmenero J. Relationship between the time-domain Kohlrausch-Williams-Watts and frequency-domain Havriliak-Negami relaxation functions. Phys Rev B Condens Matter. 1991;44:7306–12.